



Dynamic distributed drainage implied by the flow evolution of the 1996–1998 Adventure Trench subglacial lake discharge

Sasha P. Carter^{a,b,*}, Donald D. Blankenship^b, Duncan A. Young^b, Matthew E. Peters^{b,c}, John W. Holt^b, Martin J. Siegert^d

^a Institute for Geophysics and Planetary Physics (IGPP), Scripps Institution of Oceanography (SIO), University of California San Diego (UCSD), 9500 Gilman Drive, mail code 0225, La Jolla, CA 92093-0225, USA

^b University of Texas John A. and Katherine G. Jackson School of Geosciences, Institute for Geophysics (UTIG), J.J. Pickle Research Campus, Bldg. 196; 10100 Burnet Road (R2200), Austin TX 78758-4445, USA

^c The University of Texas at Austin, Applied Research Laboratories, ARL-Environmental Science Group, PO Box 8029 Austin, TX 78713, USA

^d School of GeoSciences, The University of Edinburgh, Grant Institute, The King's Buildings, West Mains Road, Edinburgh, EH9 3JW, Scotland, United Kingdom

ARTICLE INFO

Article history:

Received 1 August 2008

Received in revised form 21 February 2009

Accepted 10 March 2009

Available online 26 April 2009

Editor: M.L. Delaney

Keywords:

East Antarctica

subglacial lakes

jökulhlaup

radar

Adventure Subglacial Trench

hydrology

ice–ocean interactions

polar science

remote sensing

climate change

sea level

ice shelf

cryosphere

ABSTRACT

The transport of subglacial water beneath the East Antarctic Ice Sheet is an enigmatic and difficult to observe process which may affect the flow of the overlying ice and mixing of the oceans in the sub ice shelf cavities, and ultimately global climate. Periodic outbursts are a critical mechanism in this process. Recent analysis of satellite data has inferred a subglacial hydraulic discharge totaling 2 km³ traveling some 260 km along the ice-bed interface of the Adventure Subglacial Trench between 1996 and 1998 (Wingham et al., 2006). Rapid discharge connects Antarctic subglacial lakes. Nature 440, 1033–1036). Using radar echo sounding data from the Adventure Subglacial Trench region in conjunction with the previously reported satellite observations, along with some basic modeling, we calculate a mass budget and infer a flow mechanism for the 1996–1998 event. The volume released from the source lake exceeded the volume received by the destination lakes by ~1.1 km³. This discrepancy indicates that some water must have escaped downstream from the lowest destination lake from 1997 onward. The downstream release of water from the destination lakes continued until at least 2003, several years after the 1998 cessation of surface subsidence at the source lake. By 2003 a total of 1.5 km³ or nearly 75% of the water released by the source lake had traveled downstream from the destination lakes. The temporal evolution of discharge from the outlet can be simulated with the classic ice-walled semicircular channel model, if and only if the retreat of the source lake shoreline is taken into account. Further downstream, the ice bedrock geometry along the inferred flow path downstream includes many sections where thermal erosion of the overlying ice would not be sustainable. Along these reaches mechanical lifting of the ice roof and/or erosion of a sedimentary substrate by a broad shallow water system would be most effective means of sustaining the discharge. A distributed system is also consistent with the 3-month delay between water release at the source lake and water arrival at the destination lake. Observations of intermittent flat bright bed reflections in radar data acquired along the flow path are consistent with the presence of a broad shallow water system. Ultimately the presence of large subglacial lakes along the flow path of the 1996–1998 Adventure Subglacial Trench flow path delayed the arrival of water to points downstream by approximately 12 months.

© 2009 Elsevier B.V. All rights reserved.

1. Overview

Subglacial water movement in Antarctica causes rapid ice-surface elevation change that can be detected through repeat satellite altimetry and synthetic aperture radar interferometry (Gray et al.,

2005; Wingham et al., 2006; Fricker et al., 2007). The water systems themselves, including both the reservoirs and the channels, can be observed through radar echo sounding (henceforth RES; Siegert et al., 2005; Carter et al., 2007) and seismic reflection (Peters et al., 2007). Numerous models have been used to describe the evolution of subglacial water during a subglacial flood (e.g., Björnsson, 1992; Ng, 2000; Clarke, 2003, 2005). However, these models have generally been adapted to temperate glacier systems on relatively steep mountains, where discharge emerges into an open lake or river (Roberts, 2005). Water transport models for Antarctica generally have assumed either steady discharge (e.g., Johnson, 2002; Le Brocq et al., 2006) or local water supply (e.g., Tulaczyk et al., 2000; Bougamont

* Corresponding author. Institute for Geophysics (UTIG), J.J. Pickle Research Campus, Bldg. 196, 10100 Burnet Road (R2200), Austin TX 78758-4445, USA. Tel.: +1 512 471 0418; fax: +1 512 471 0999.

E-mail addresses: spcarter@ucsd.edu (S.P. Carter), blank@ig.utexas.edu (D.D. Blankenship), duncan@ig.utexas.edu (D.A. Young), peters@arlut.utexas.edu (M.E. Peters), jack@ig.utexas.edu (J.W. Holt), M.J.Siegert@ed.ac.uk (M.J. Siegert).

et al., 2003). Recently it has been demonstrated that episodic water flow may lead to enhanced flow of the overlying ice (Stearns et al., 2008). Understanding the distribution and dynamic behavior of subglacial water systems is essential in assessing the near-term behavior of the overlying ice sheet. (Blankenship et al., 2001; Vogel and Tulaczyk, 2006; Bell, 2008). Furthermore, as subglacial floods reach the ocean they could constitute a major point source of cold freshwater, which, at a minimum, alters water circulation in the sub-ice-shelf cavity and therefore alters freezing and melting on the base of the ice shelf. At a maximum, the release of freshwater may alter global ocean circulation (Payne et al., 2007).

A study of European Remote Sensing Satellite 2 (ERS-2) radar altimetry documented an ice-surface subsidence event of 3 m that began in late 1995 over a previously unknown subglacial lake in the Adventure Subglacial Trench (AST), in central East Antarctica (Wingham et al., 2006). This subsidence coincided with a surface inflation of

approximately 2 m over a known subglacial lake 260 km away. An analysis of bed topography led Wingham et al. (2006) to conclude that the surface changes were caused by a unique water-flow event. Using complimentary Interferometric Synthetic Aperture Radar (InSAR) observations they calculated that the source lake, hereafter referred to as “Lake L,” had a surface area of 600 km². Assuming uniform subsidence over the lake, they determined that nearly 1.8 km³ of water was released from Lake L (Wingham et al., 2006; Figs. 1 and 2). From observations of the surface motion, ice thickness, and bed elevations at the two major lakes, the authors suggested that water may have been transported via a semicircular conduit incised into the ice directly above the bed. Although such a mechanism has been observed in relatively steep, temperate subglacial environments (Röthlisberger, 1972) it is not immediately apparent whether such a system is stable over the relatively long distances and shallow slopes associated with a continent-wide ice sheet (Alley, 1989). Occurring

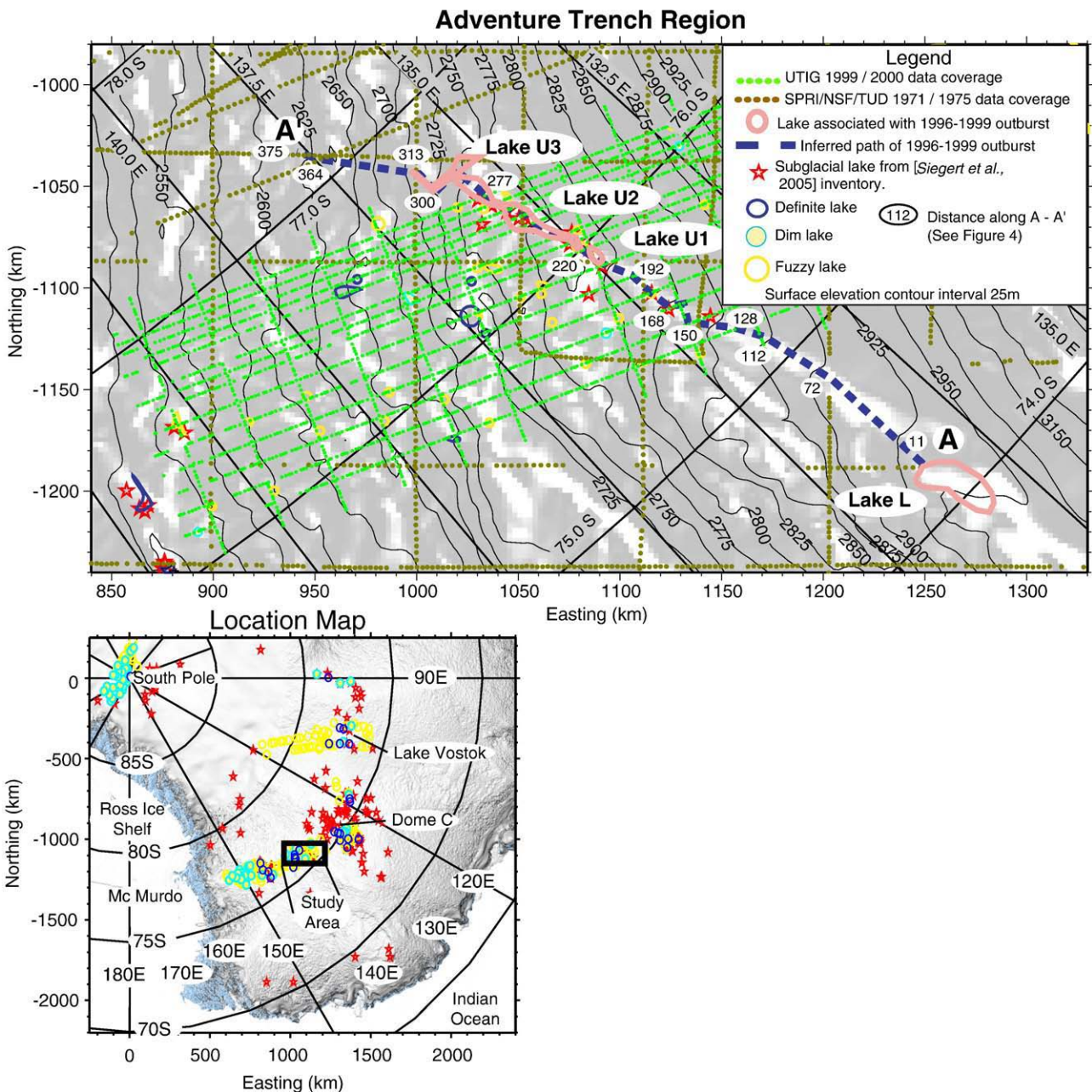


Fig. 1. Overview map of Adventure Subglacial Trench region, showing coverage of available radar sounding data, relevant subglacial lakes, ice surface topography, and the inferred flow path of the 1996–1998 Adventure Subglacial Trench discharge. Map background is the MODIS-based Mosaic of Antarctica (MOA) (Scambos et al., 2007).

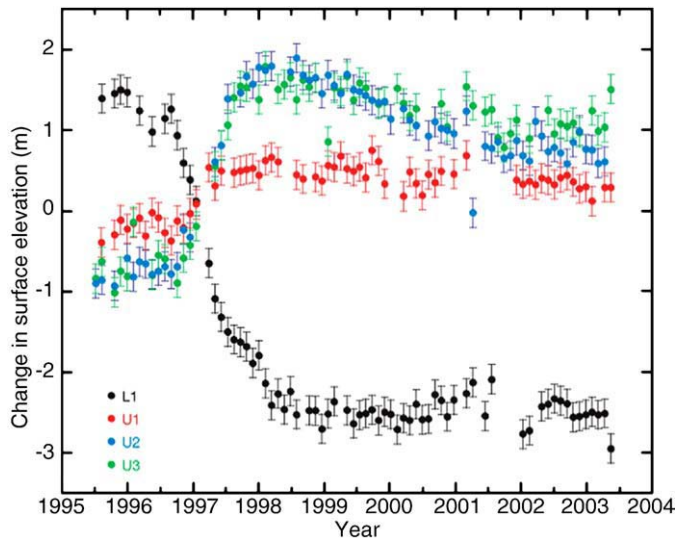


Fig. 2. Surface height change from 1996–2003 from ERS-2 radar altimetry at Lake L, the source lake and Lakes U1, U2, and U3, the destination lakes from the article From the following article: “Rapid discharge connects Antarctic subglacial lakes.” Duncan J. Wingham, Martin J. Siegert, Andrew Shepherd and Alan S. Muir, *Nature* 440, 1033–1036 (20 April 2006) doi:10.1038/nature04660. ©2006 Nature publishing group. Reprinted with permission.

nearly 700 km from the nearest coastline, the 1996–1998 AST discharge originated further inland than any documented subglacial flood to date and may still hold the record for the greatest distance traveled by any single documented subglacial flood in Antarctica (e.g., Goodwin, 1988; Denton and Sugden, 2005; Gray et al., 2005; Fricker et al., 2007; Stearns et al., 2008). The Adventure Trench subglacial flood and other potential outbursts in the Antarctic interior may be a vital means of transporting water produced and stored under the relative insulation and stability of the ice divide regions to the onsets of fast glacier flow (Bell, 2008). In this work, we use airborne RES data from the inferred flood path in conjunction with the previously published surface elevation data to construct a mass budget for this flood, infer a flow mechanism, and determine whether the discharge traveled beyond the last destination lake.

2. Data/methods

2.1. Satellite coverage of the AST lakes

Observations of the topography and motion of the ice surface play a crucial role in understanding the distribution and behavior of water at the base of the ice. In addition to the InSAR-derived motion for Lake L and the ERS-2 repeat and crossover radar altimetry used by Wingham et al. (2006), we use two other data sets on surface texture and topography to characterize the recent discharge: the Moderate Resolution Imaging Spectroradiometer Mosaic of Antarctica (MODIS MOA) (Haran et al., 2005; Scambos et al., 2007) and the Geoscience Laser Altimeter System/Ice Cloud and land Elevation Satellite Digital Elevation Model (GLAS/ICESat DEM) (DiMarzio et al., 2007).

The MODIS MOA imagery has been used to identify and characterize large subglacial lakes based on patterns in the surface of the overlying ice (Bell et al., 2006, 2007). Collected between November 2003 and February 2004, this imagery seamlessly blends hundreds of cloudless digital images of the ice surface to create a map of Antarctica in which the continent appears to be illuminated by a distant light originating from approximately 45° E (Haran et al., 2005;

Scambos et al., 2007; Fig. 3). The 750 m spatial resolution of this data set provides detailed information about the texture of the ice surface, capturing most major ice-flow features and surface lineations. On the MODIS MOA imagery these locations will appear as “flat” with a consistent brightness across the region. The shoreline will take on the appearance of a bright line for half its length, with a thin shadow defining the remainder of the lake edge (Bell et al., 2006, 2007; Fig. 3). This effect due to the substantially lowered ice surface slopes associated with subglacial lakes relative to their surroundings as caused by the absence of basal friction at the ice–water interface (Ridley et al., 1993; Pattyn, 2003; Remy and Legresy, 2004; Fig. 3).

In order to observe the slope anomalies found in MOA in a more quantitative fashion and obtain consistent data for our calculation of hydraulic head (discussed next section), we supplement the texture resolution of the MODIS MOA with the accurate satellite laser altimetry of the GLAS ICESat DEM. This data set was created from gridding and interpolating between the laser altimetry profile measurements made by the ICESat missions between February 2003 and June 2005 (DiMarzio et al., 2007). Although the resolution of this data set approaches 0.5 km near 86° S, aliasing effects arise when data is gridded to this resolution farther north, as it would be at our study area near 74° S (Bamber and Gomez-Dans, 2005; Shuman et al., 2006). To address this aliasing we selected a cell size of 2.5 km² when gridding the ICESat DEM and then applied a 5 km isotropic 2-dimensional Gaussian filter to the gridded data.

To identify subglacial lakes in the ICESat DEM we use a surface-altimetry-processing technique presented by Remy and Legresy (2004) and Smith et al. (2006) that compares the local surface to the regional surface slope. This involves comparing the surface slope on the original surface elevation map to the surface slope on a map of the same data gridded to 10 km and filtered to 50 km. The resulting map shows surface texture in a manner similar to MOA, except that the apparent lighting direction for any point is always appears to originate from up the regional surface slope. In this map possible subglacial lakes appear always appear bright relative to their surroundings (2006; Supplementary Information 1) to produce a map of surface slope anomalies (Fig. 3). This technique is however limited in use due to the non-uniqueness of surface anomalies to subglacial lakes (Pattyn, 2003). Surface anomalies may also be produced by bedrock topography or the transition between stuck and sliding ice. A further discussion on these limitations is included in our error calculations.

2.2. Radar sounding coverage of the AST lakes

RES is the primary method by which the dimensions and properties of subglacial lakes and the waterways that connect them can be determined. Two airborne RES data sets cover the AST region: The 1998–2000 University of Texas Institute for Geophysics (UTIG) RTZ9 campaign and the NSF/Scott Polar Research Institute/TU Denmark (SPRI) campaigns of 1971–72 and 1974–75 (Drewy, 1975), which are included in the BEDMAP database of subglacial topography (Lythe and Vaughan, 2001).

The RTZ9 survey covers a 120-km wide corridor with flight lines 5–10 km apart (Fig. 1). This region includes all of the destination lakes (Lakes U1, most of U2, and part of U3) but excludes Lake L (Richter et al., 2001; Carter et al., 2007). The RTZ9 RES data provide detailed basal topography, basal reflectivity, and reveal the structure of the ice overlying the ice–bedrock interface (Table 1; Fig. 4). The serendipitous timing of this survey, less than 2 yr after the 1996–99 drainage event, provides a snapshot of the recently altered subglacial landscape. Flight lines from the SPRI campaigns of 1971–72 and 1974–75 supplement our

Fig. 3. a) Schematic diagram of how “lakes” appear as bright ice surface reflections in MODIS imagery. The MODIS Mosaic of Antarctica image selected only images that were lit from 45° E to maintain consistency. b) MOA mosaic for area shown in Fig. 1 with lakes involved in the discharge and other lakes. Arrows indicate direction of “lighting.” c) GLAS/ICESat DEM processed to reveal flat surface anomalies as shown in a). Arrows indicate lighting direction.

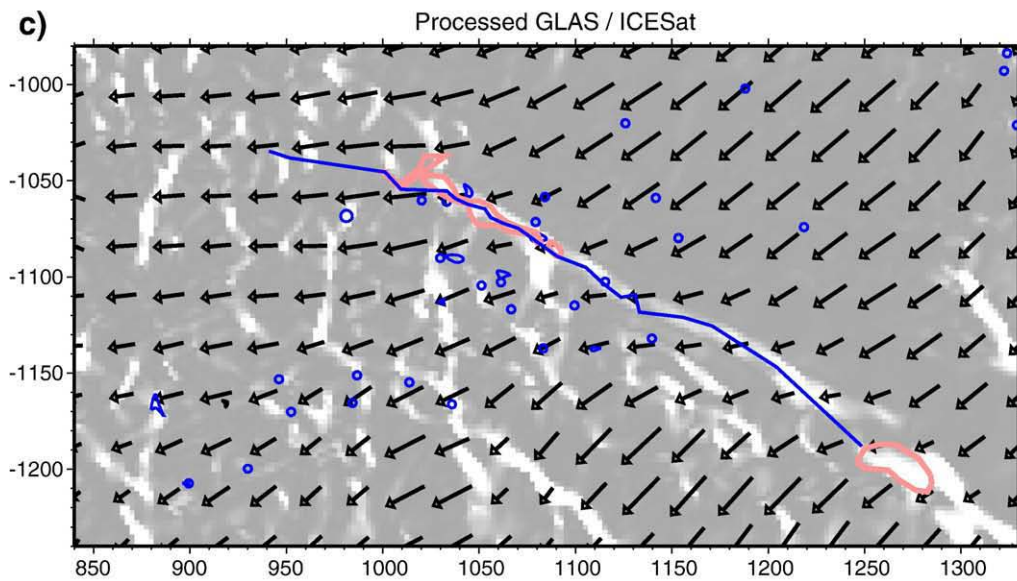
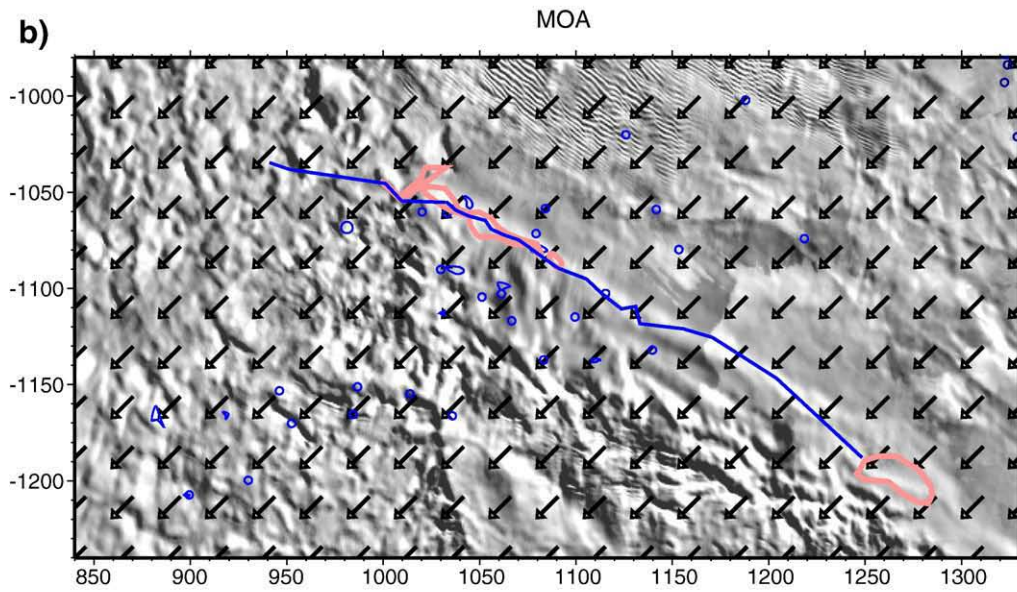
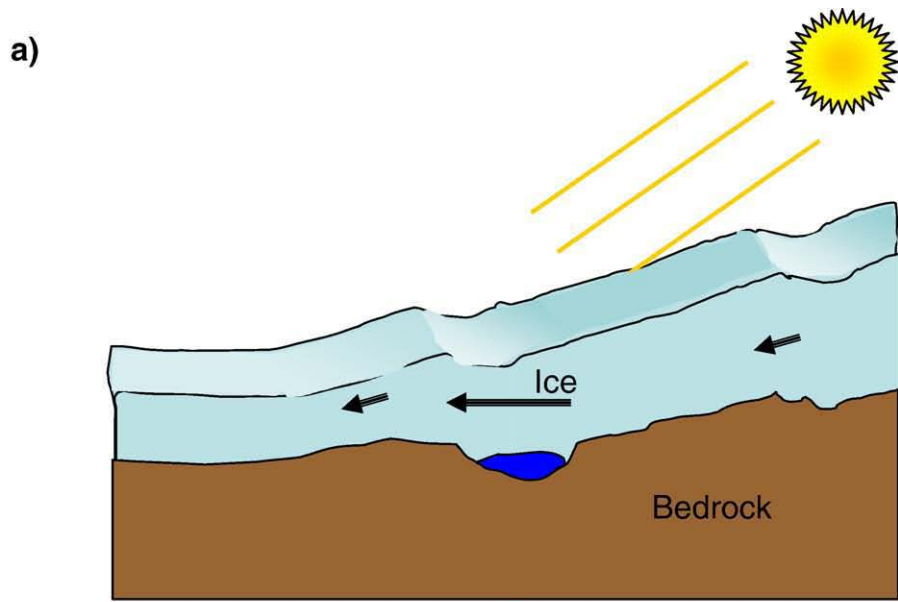


Table 1
Side-by-side comparison of SPRI and UITG airborne radar data.

Survey name	1999–2000 UTIG RTZ9	SPRI 1971/72 and SPRI 1974/75
Dates	1999–2000	1971–1975
Sample spacing	10–12 m	~3 km
Main line spacing (km)	5–10	25
Tie-line spacing (km)	30	50
Ice reference surface used here	Laser/radar altimetry	ICESat DEM
Aircraft	DeHavilland Twin Otter	C130 Hercules
Thickness logging method	Digital	35 mm film
Navigation	GPS	Inertial navigation
Navigational precision	10 cm	3 km
Thickness procedure	169 m/μs no firm correction	168.5 m/μs + 15 m firm correction

knowledge of the bedrock topography outside the area covered by the RTZ9 survey and provide a perspective on the destination lakes (U1, U2 and U3) before the 1996–98 discharge (Table 1). The surface elevation in RTZ9 data is obtained by onboard GPS and the two-way travel time of the signal from the plane to the ice. The surface elevation for the SPRI data is obtained from the previously described ICESat DEM. Using line data instead of the BEDMAP grid enables us to gain a more accurate picture of the hydrologic head so that we can evaluate the most likely path water will take at the base of the ice sheet and avoid treating artifacts in the interpolated BEDMAP topography as real. The hydrostatic head of water, equal to the sum of the water elevation head and water pressure head at the base of the ice, is calculated assuming that water pressure is equal to the ice overburden pressure through the formula:

$$h_h = z_{srf} - (1 - \rho_{ice} / \rho_{water}) * h_{ice} \quad (1)$$

where:

h_h	the hydrologic head
z_{srf}	the ice surface elevation
ρ_{ice}	the density of ice
ρ_{water}	the density of water; and
h_{ice}	the ice thickness

The resulting calculation reveals the hydrologic topography of the region, with water flowing along the valleys in head and collecting in the local hydraulic minima (Fig. 5). The initial or base hydraulic gradient is obtained from simply connecting and correlating the local minima in the hydraulic head along each flight line and dividing the head difference by the distance (Fig. 6).

We locate lakes within the area covered by either RTZ9 or SPRI data using a lake-classification algorithm (Carter et al., 2007). This algorithm identifies continuous sections of a flight line of 500 m or longer where the apparent slope in the hydraulic head is less than 0.1%, placing the shoreline at the point where this slope begins to exceed 0.1%. The shore points are then arranged to form an irregular polygon, with the shoreline equivalent to its perimeter (Fig. 4).

2.3. From altimetry and ice-penetrating radar to hydrographs

We obtain filling and drainage rates for the AST subglacial lakes through multiplying the temporal change in surface elevation with time by the lake area (Fig. 2). In this calculation we assume that lake area remains constant with volume and that subsidence / uplift is uniform over the entire lake surface. The error associated with this assumption is discussed in the next section. From a discharge versus time graph we are able to compare the timing of hydraulic release from Lake L and the arrival of water in the destination lake (U1, U2 and U3). Knowledge of

the timing enables us to assess the prospect of leakage from the destination lakes and infer a possible flow mechanism (Fig. 7).

2.4. Possible sources of error for mass budget

The three sources of error in the mass budget come from imprecision in the satellite altimetry, uncertainty about the shoreline, and the neglect of the effects of ice flexure near the lake shoreline. Wingham et al. (2006) state that the error associated with the ERS-1 and the ERS-2 satellite altimetry is ± 0.18 m per measurement. Since a measurement of elevation change must incorporate two surface elevations, the RMS error is 0.25 m. As the magnitude of this error exceeds the surface accumulation rate by an order of magnitude (Arthern et al., 2006) and the estimated basal melt rate by two orders of magnitude (Johnson, 2002), we treat errors associated with these two phenomena as negligible. Uncertainty with regards to the shoreline depends on whether there is sufficient RES coverage over a given lake. Where such coverage surrounds the lake we have calculated the variability associated with flight-line data gaps to be approximately 10% of the lake volume. This figure is based on an in-house comparison of the area for Lake Vostok using all the known shore points and using only a regular subset of known the lake's shore points (See supplementary information). It was found that sampling errors could affect the lake's area by approximately 10%, assuming that the overall shape of the lake is not distorted by the data gaps (Fricker and Scambos, 2009). For lakes larger than a few square kilometers, this figure is an order of magnitude larger than the ~150 m error associated with locating the shoreline within the radar profiles (Carter et al., 2007). For lakes or portions where the area is determined solely from static surface anomalies, we have to factor in the non-uniqueness of surface slope anomalies to subglacial lakes. Both slippery saturated sediments and the transfer of bedrock topography to the surface can produce lake-like surface anomalies. Even in locations where a surface slope anomaly is associated with a subglacial lake, recent modeling work suggests that the aerial extent of the anomaly may greatly exceed the area of the actual lake because of the response of the flowing ice to an abrupt change in basal traction (Pattyn, 2003; Sergienko et al., 2007). For these reasons we estimate an error of 50% for the area of any lake or lake portion identified solely from surface anomalies.

The assumption of uniform uplift across the lake surface may constitute our greatest source of systematic error for the mass budget. As the release of water from a subglacial lake outlet lowers the pressure in the lake that was previously available to support the ice roof, some of the associated strain will be taken up by flexure of the adjacent ice, such that the concavity of the ice surface increases over the lake (Evatt and Fowler, 2007). For a circular lake of sufficient depth, the profile will be roughly parabolic. If the shoreline is interpreted as lying at the edge of area of vertical surface deformation and the effect of ice flexure is neglected, the calculated volume-change estimate may be a factor of two greater than the actual volume change, if surface height change is measured at the lake center. Substantial mitigation to such error is accomplished by the earlier described method of basing our shoreline position on the hydraulic gradient, thereby eliminating these edges from consideration in our volume change calculations (Carter et al., 2007). Furthermore surface height is measured not at the point of maximum drawdown, but represents a spatial average over the footprint of the crossover area (Arthern et al., 2001; Wingham et al., 2006). Additionally if we consider some portion of the error to be systematic across all lakes involved in the discharge, the relative magnitude can be reduced, making our final estimate equal to approximately 12% of the lake volume for a given lake.

Given that the bedrock slope along the valley sides exceeds 1% throughout Adventure Trench, we do not account for lake area change over the course of the flood, as a 1% slope will result in a shoreline position change of less than a few hundred meters as the

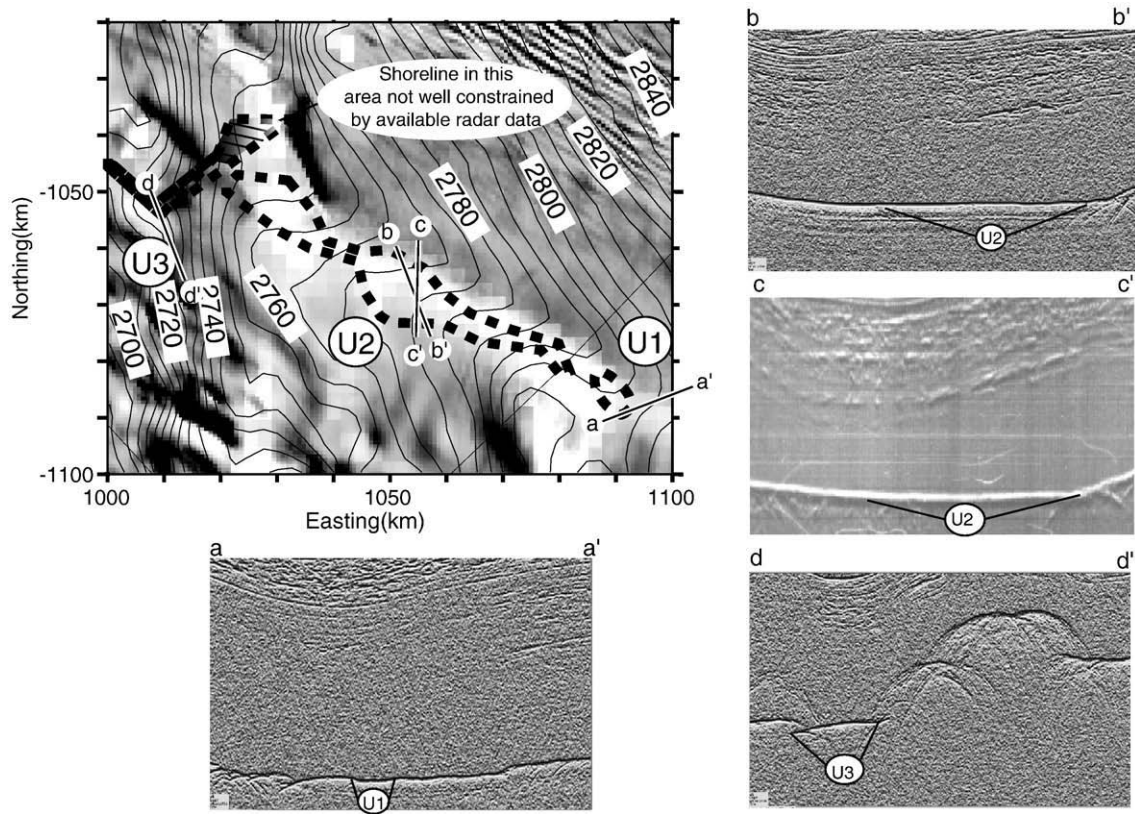


Fig. 4. Detailed map and radar profiles of the destination Lakes U1, U2, and U3. All images except for c–c' are from the 1999/00 UTIG data. c–c' is from the 1974/75 SPRI radar inventory. All figures represent approximately 15–20 line km of data and 2000 m of height. Amplitudes in these images are from differentiated data.

lake fills or drains. Along the trench axis, where the bedrock slope is less than 0.05%, a subglacial lake's shoreline could advance/retreat several kilometers over the course of filling/draining (Evatt et al., 2006). The fuller implications of shoreline movement are discussed in the modeling section.

2.5. Using hydraulic head, discharge and topography to model a flow system

2.5.1. Features common to both models

Using the detailed information on bedrock elevation, ice surface elevation, and the corresponding hydraulic head along the flow path

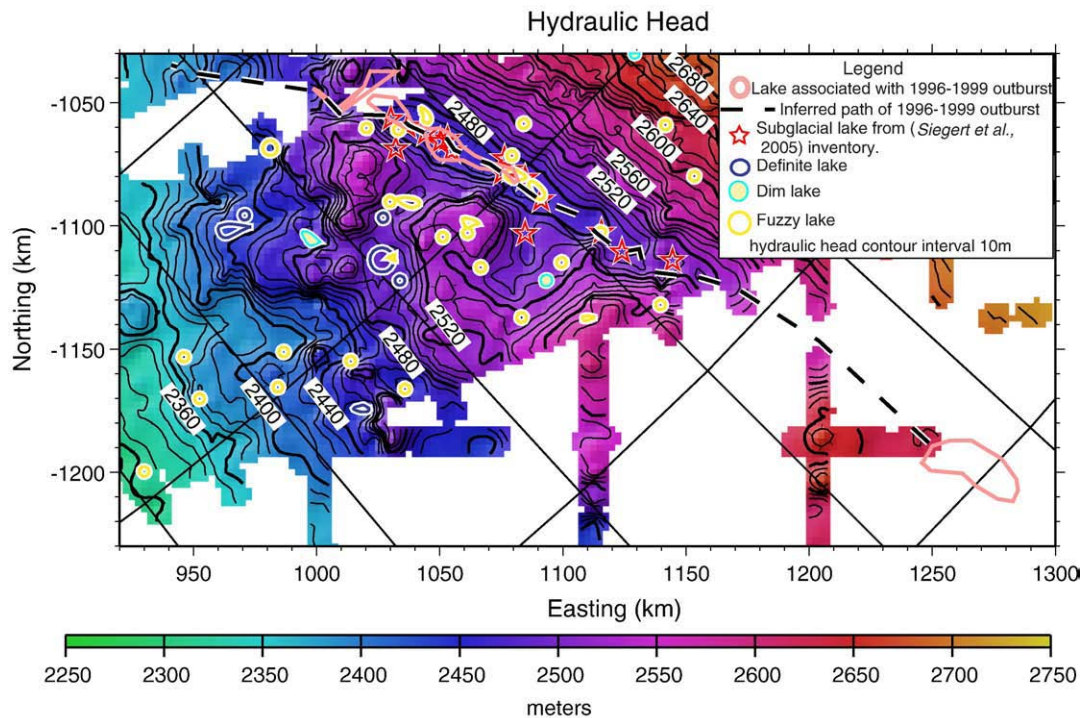


Fig. 5. Radar derived hydraulic head for the Adventure Subglacial Trench and its surroundings.

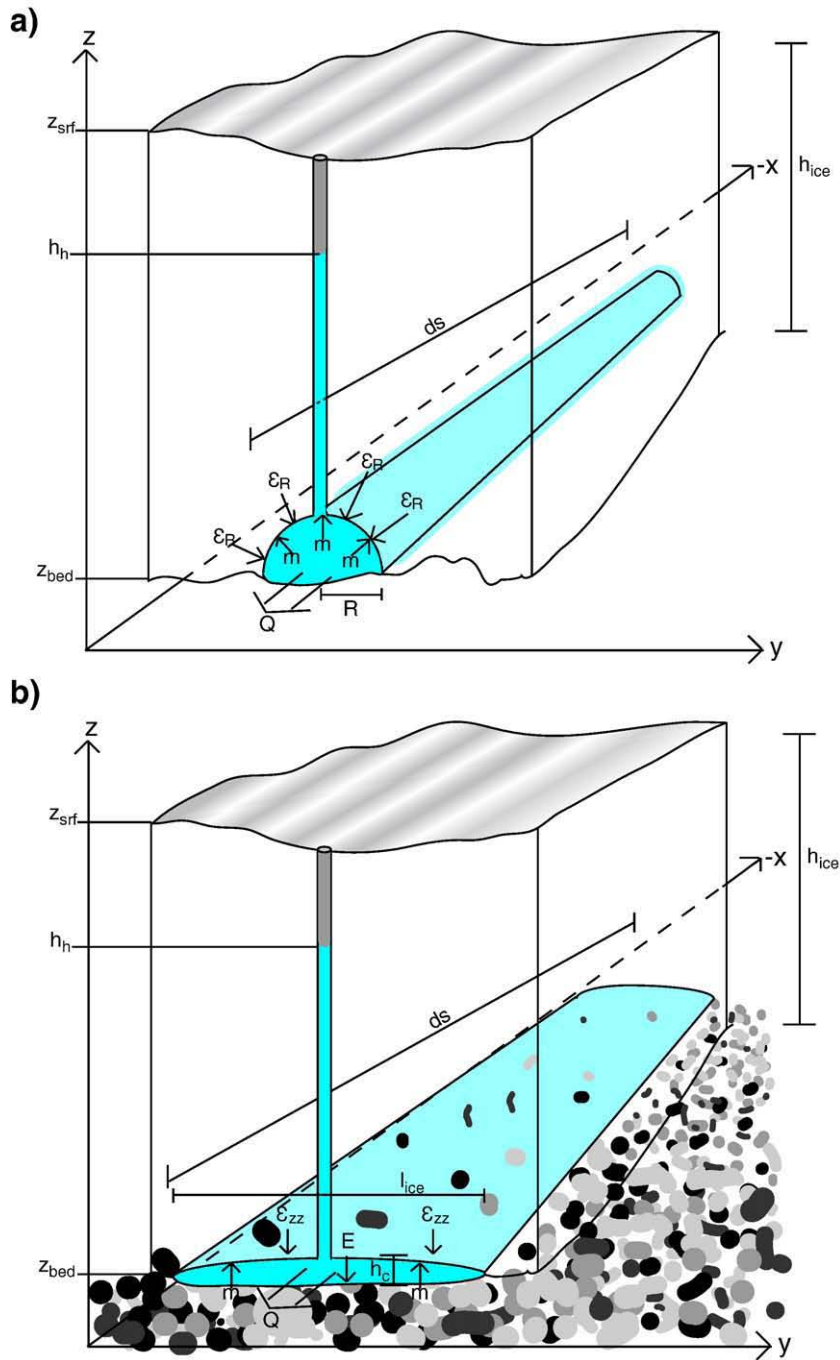


Fig. 6. Schematic diagram of a) the semicircular conduit model used in this study (Röthlisberger, 1972; Nye, 1976) and b) broad shallow canal used in this study (Walder and Fowler, 1994). Figure is not to scale.

obtained from the RES profiles along with the calculated rates of volume change for the source and destination lakes we construct two models for the water system in Adventure Trench. In contrast to other modeling efforts (e.g., Johnson et al., 2002; Le Brocq et al., 2006), which use the BEDMAP grid for ice–bedrock topography, our use of the original radar profile data allows resolution of critical topographic details along the flow path and eliminates interpolation-related artifacts (Fig. 5). This in turn allows a more accurate calculation of the gradients of hydraulic head, ice surface elevation, and bedrock elevation, though dividing the change in these measurements over the distance between each measurement point. These models address the initiation, evolution, and fate of discharge from Lake L, identifying which proposed flow systems may be stable and the affect such flow systems may have on the overlying ice. In modeling we do not

consider a porous media aquifer or a thin film at the ice bed interface as neither is capable of transporting even a fraction the inferred discharge along the hydraulic gradient from the source lake to the destination lake (Alley, 1989). Therefore we model two higher-capacity systems: semicircular conduits and broad, shallow canals.

In testing the stability of the two flow systems one of the most important considerations is the thermodynamic behavior. It has been hypothesized that subglacial lakes are most likely to occur immediately upstream of locations where water flowing down the hydraulic gradient encounters an adverse bed slope greater than twice the surface slope (Clarke, 2006). Along such reaches the pressure melting point for water flowing downstream will increase more rapidly than heating from viscous dissipation can raise the temperature (Alley et al., 1998). In such locations, water will tend to

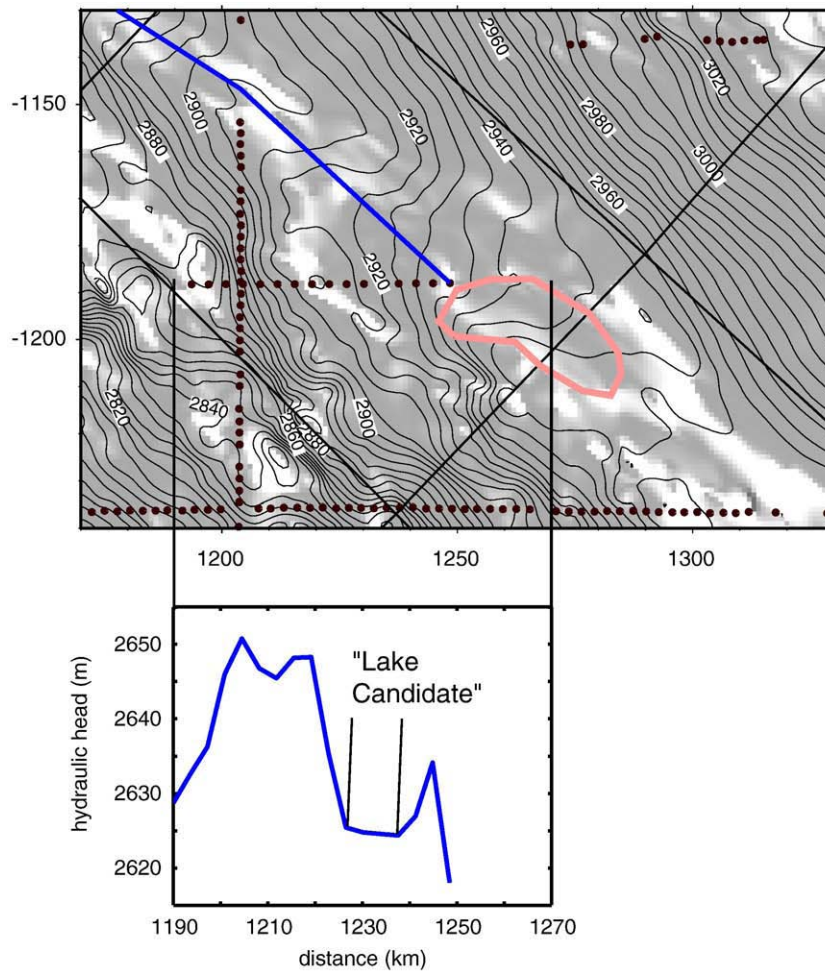


Fig. 7. Large scale map of surface anomalies around Lake L, with inset showing hydraulic head along nearest radar sounding profile.

freeze out and accrete onto the base of the ice if sufficient nuclei are present. The significance of these details is that the ice surface and bedrock topography exert a primary control on the ability of subglacial water to melt a passage through the overlying ice in this environment.

In addition to the test of thermodynamic stability we also test the previously mentioned effect of shoreline retreat on the evolution of discharge from the source lake. At the source lake hydraulic head, surface elevation, and ice base elevation all decrease with the cumulative discharge. To test the effect of shoreline retreat during this process, we allow the distance between the point in our model representing Lake L and the point immediately downstream of Lake L to increase as the lake lowers. It is expected that water will be traveling up an adverse bed slope in such a situation and may also be originating from under increasingly thick ice as the shoreline retreats. As the bathymetry of Lake L is not well-known, we assume a linear bedrock slope at the outlet and a continuous ice-surface slope. It is also likely that the filling of the destination lake will cause the shoreline to expand up and down the valley, though this effect is not dealt with explicitly in our model.

2.5.2. Semicircular conduits (*R*-channels)

The Röthlisberger channel, or *R*-channel, model describes a semicircular conduit at the ice-bed interface, with discharge increasing both with conduit diameter and effective hydraulic gradient (Fig. 6). Expansion of the conduit is accomplished through melting of the conduit walls by the viscous dissipation of kinetic energy in the water as it moves down

the hydraulic gradient. Conduit closure occurs through viscous deformation of the conduit walls because the pressure of the ice exceeds the pressure in the conduit (Röthlisberger, 1972; Nye, 1976; Supplementary Information II). Although this channel is essentially similar to the model used by Wingham et al. (2006) in their description of the 1996–98 discharge, our model includes increased spatial and temporal resolution. Whereas the original model only included the two endpoints, our model includes a number of intermediate points obtained from RES data. This allows us to assess the behavior of water at intermediate points and identify where such a system may not be stable. The time-varying component allows direct comparison between modeled and observed discharge. This model benefits from being relatively simple and requiring only inputs that have been directly measured. The major drawback to this model comes from its assumptions on conduit shape and neglecting the effects of water-bed interactions.

2.5.3. Broad-shallow canals

A review of the literature on the transport of subglacial water indicates that in areas of low hydraulic gradient, such as the interior of a continental ice sheet or ice streams, broader systems with a lower ceiling may be more stable (Kamb, 1987; Alley, 1989; Hooke et al., 1990; Catania and Paola, 2001). In choosing such a system to model, we considered not only the details with which a model is required to operate, but also the appropriateness of a model to the given data, as a model that requires too much knowledge of the underlying basal material would be made irrelevant by the lack of data (Fowler and Ng, 1996; Ng, 2000). We assume the presence of unconsolidated

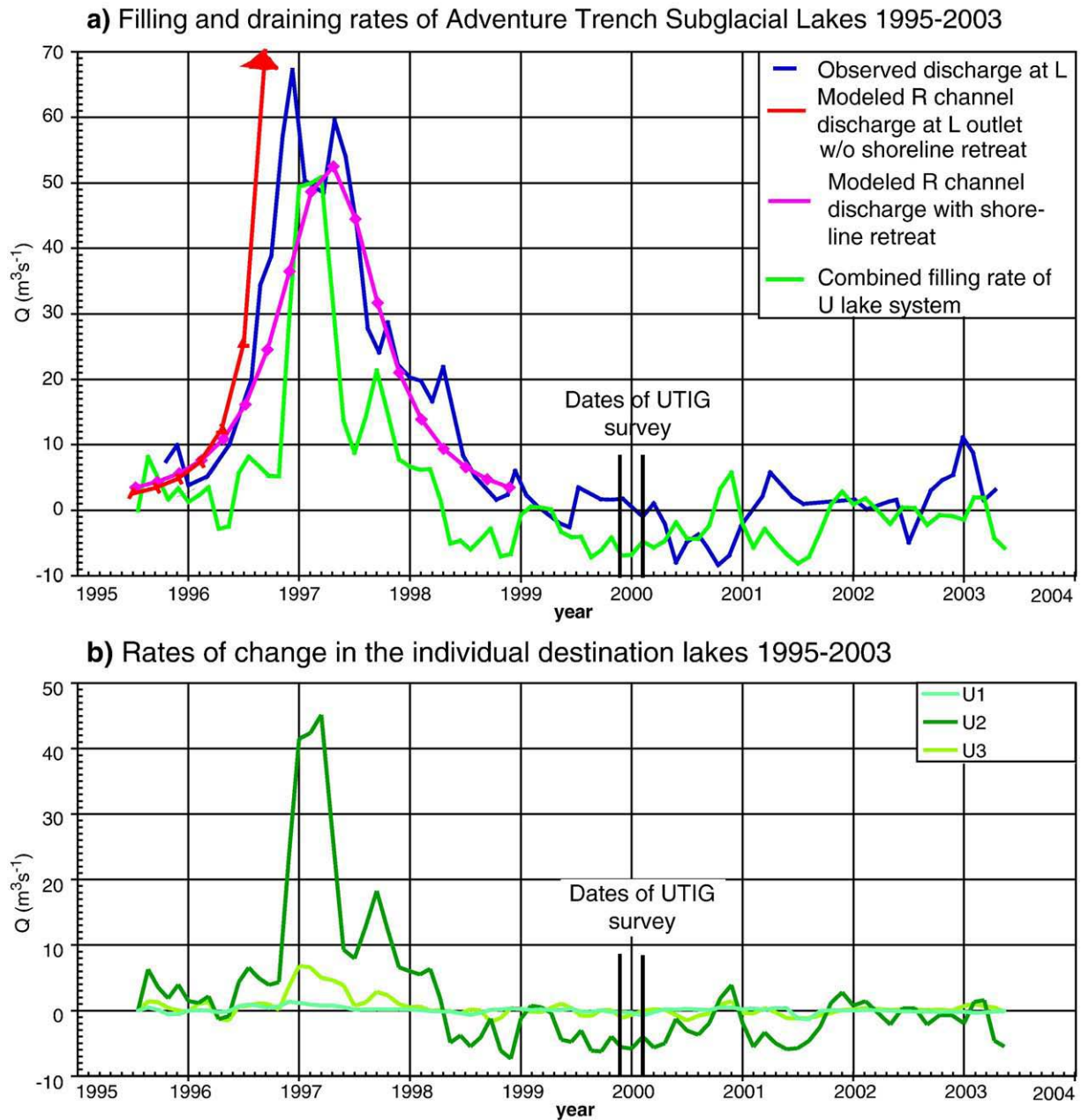


Fig. 8. Rates of volume change for a) the source (L) and destination (U1, U2 and U3 combined) lakes b) individual destination lakes. The values are derived by taking the derivative of the lake surface elevation (Wingham et al., 2006) with respect to time and multiplying that time derivative by lake area. Positive values for L correspond to volume loss. Positive values for U1, U2, and U3 correspond to volume gained.

sediments on the basis of two separate aerogeophysical campaigns over the AST, in which both teams identified a 10 km thick sedimentary basin through analysis of gravity anomalies and magnetic anomalies in the region (Ferraccioli et al., 2002; Studinger et al., 2004). Sediment size is inferred from sediment collected from several West Antarctic ice streams in which median particle size ranged between 120 and 250 μm (Tulaczyk et al., 1998). Although a number of the above mentioned models and data are associated with West Antarctic ice streams, Adventure Trench region, like much of West Antarctica, has a low ice surface and bedrock gradient and is probably underlain by marine sediments deposited before the onset of glaciation in the region (Evatt et al., 2006).

The resulting model, described in more detail in [Supplementary Information III](#), uses the equations put forth in [Walder and Fowler \(1994\)](#). This model loosely describes a broad, shallow canal carrying both

sediment and water over a deformable bed. The cross-sectional geometry of this waterway is controlled not only by discharge and the hydraulic gradient, but also by the size of the sediments. Using the previously determined flow-path geometry, the discharge from the source lake, and inferred sediment distribution, we use the model to estimate, canal dimensions, effective pressure in the canals, travel time, and instantaneous rate of growth/contraction of the canal cross section associated with the deformation and erosion of the overlying ice and underlying sediments. We interpret shutdown in this model as occurring by one of two processes: accretion of ice onto the canal roof (Alley et al., 1998) or creep closure through viscous deformation of the ice roof and underlying sediments (Fowler and Ng, 1996; Hooke, 1998). The major drawback to this particular model as presented in [Walder and Fowler \(1994\)](#) is that canal height is made to be entirely a function of sediment grain size and hydraulic gradient while neglecting discharge. For this reason, we limit

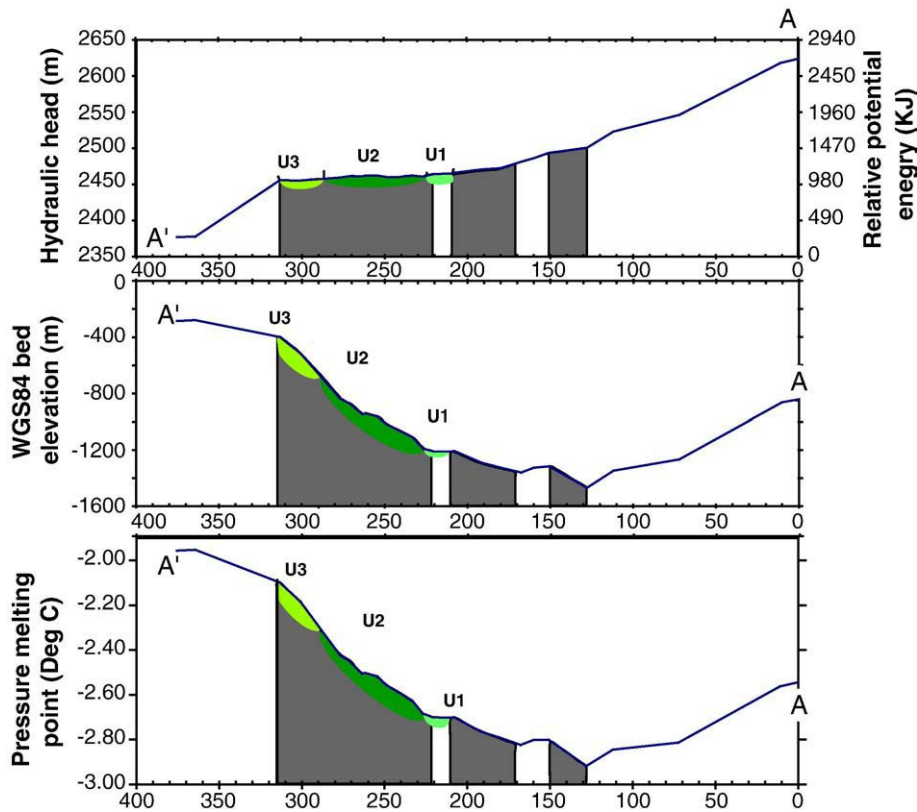


Fig. 9. Hydraulic head, bed elevation and the pressure melting point of basal ice along the transect A–A' (see Fig. 1). Gray shading indicates areas where thermal erosion would not be possible. Even with the relatively sparse sampling here it is apparent that the assumptions concerning an idealized straight flow path are not valid. The route contains numerous rough spots.

the use of this model to testing the viability of a distributed system rather than exploring its full evolution over the course of the flood.

3. Results

3.1. Lake descriptions

3.1.1. Lake L

Lake L, the source lake for the 1996–98 AST discharge, has a published extent of 600 km² (Wingham et al., 2006). Although the flat trace of L is difficult to distinguish in the MOA, the slope anomaly processed ICESat DEM reveals a bright area nearly coincident with the previously published lake shoreline (Fig. 8). The aerial extent by this

shoreline is approximately 490 km². If we determine area from the published InSAR imagery, then the maximum possible extent for the lake is 730 km². Although no radar images are available for L, one survey line from the SPRI survey crosses the southern end of the lake near the outlet (Fig. 8). The portion of this line closest to Lake L is hydraulically flat, consistent with the presence of water (Fig. 8). We use the hydraulic head along this portion of the flight line to infer the hydraulic head and ice thickness across the rest of L using our outline and the ICESat DEM and Eq. (1). Through this calculation we infer that the ice thickness over Lake L ranges from 3475 m to 3950 m, while ice-base elevation varies between –560 and –1000 m. Our calculations for area and elevation change estimate a total volume released of 2.24 ± 0.50 km³ and a maximum discharge of 66.0 ± 14.7 m³s⁻¹ (Fig. 9; Table 2). The Wingham et al. (2006) release estimate of 1.8 km³ and estimated discharge of 50 m³s⁻¹ both fall near the bottom of our error bounds. Given the paucity of RES data from directly over the lake, we treat our estimate and the Wingham et al. (2006) estimate as essentially equivalent.

Table 2
Summary of volume changes and discharge/filling rates for the AST lakes.

	Area (km ²)	Surface change (m)	Volume received (km ³)	Maximum rate of volume change (m ³ s ⁻¹)	Percentage of Lake L received
Lake L	600 ± 100	-3.74 ± 0.25	2.24 ± 0.50	66.2 ± 14.7	100%
Lake U1	31 ± 3	1.01 ± 0.25	0.03 ± 0.01	1.4 ± 0.43	1%
Lake U2	368 ± 72	2.47 ± 0.25	0.91 ± 0.23	48.0 ± 11.9	41%
1996–1998					
Lake U3	64 ± 37	2.22 ± 0.25	0.14 ± 0.08	7.4 ± 4.19	6%
Total			1.08 ± 0.24	56.8 ± 13.1	48%
Lake U2	368 ± 72	-1.15 ± 0.25	-0.42 ± 0.20	-10.3 ± 4.85	19%
1998–2003					
Overflow	-	-	1.12 ± 0.46	-	50%
1996–1998					
Total discharged below U3	-	-	1.53 ± 0.52	-	68%

3.1.2. The destination lakes

Of the three destination lakes only U2 was classified as a “definite lake” with a continuous bright specular reflection in Carter et al., (2007). Its area of 368 ± 71 km² is over three times the combined volume of the other two destination lakes and its behavior during the flood appears to be synchronous with these two adjacent lakes. Lake U2 measures 60 km in length and 10 km across, making it a significant feature in East Antarctica. The ice thickness changes by more than 400 m from north to south. The northern end appears to be shallow, whereas depth is less certain toward the southern end (Carter et al., 2007). Both the MODIS MOA imagery and the processed ICESat DEM indicate a large surface anomaly over U2. In both data sets this anomaly extends more than 50 km north of the known lakeshore. In the southern section the

correlation between the anomaly in the processed ICESat DEM and the actual lakeshore appears to be more accurate. We use this correlation to extend the southern boundary of the lake to the limit of this anomaly (Figs. 1 and 4). With a surface rise of 2.5 ± 0.25 m, Lake U2 received up to 0.91 ± 0.23 km³, or about 41%, of the water discharged from Lake L. The maximum filling rate was 48 ± 11.9 m³s⁻¹. From the end of the discharge in 1998 to 2003, the surface of Lake L deflated by 1.15 ± 0.25 m. From this observation we calculate a total discharge of 0.4 km³ at a maximum rate of about 10 m³s⁻¹ (Fig. 9). This maximum discharge is about one-fifth of the reported discharge from Lake L (Wingham et al., 2006). Analysis of a 1974 SPRI line from this lake shows no discernable change in shoreline indicating that the lake probably holds water between floods.

Lake U1 with a surface area of 31 ± 3.1 km² is classified as a “fuzzy lake” demonstrating a bright, spatially intermittent basal reflection (Carter et al., 2007). This type of reflection, suggests a shallow lake (Gorman and Siegert, 1999), flat saturated sediments, or a sub-ice interface that has been subjected to fluting by ice flow over rougher topography upstream (Fig. 4). Lake U1 experienced only about 1 m of uplift (Wingham et al., 2006) and deflated very little, ultimately receiving about 0.03 ± 0.01 km³, or about 2%, of the total subglacial flood volume. The maximum filling rate for U1 was 1.4 ± 0.43 m³s⁻¹. This lake appears to have stopped filling while the others continued to rise (Fig. 9).

Lake U3 was discovered only after the ice surface was raised over 2 m in 1 yr during the 1996–98 discharge (Wingham et al., 2006). A reanalysis of RES data confirmed the location of observed surface motion was consistent with an ice–water interface (Fig. 4). We attribute the failure of a classification algorithm to identify this lake in previous studies to the presence of steep topography immediately adjacent to the relatively narrow lake. The steep adjacent topography also hampers identification of this lake from surface slope anomalies. At a minimum the lake is large enough to contain the areas of observed surface inflation and the hydraulically flat basal interface, about 27 km² (Fig. 4). At a maximum the lake contains all of the adjacent slope anomaly (Fig. 4), up to intersection with a radar line along which the calculated hydraulic head is significantly higher than that of the lake, about 102 km². With the above-mentioned minimum and maximum values, we assign an area for Lake U3 of 64 ± 37 km² (Fig. 9). Using the total surface inflation figure of 2.3 ± 0.25 m from 1996 to 1998 and the subsequent deflation of 0.35 ± 0.25 m from 1998–2003, we calculate a volume change of 0.14 ± 0.08 km³ at maximum rate of 7.3 ± 4.2 m³s⁻¹ (Fig. 9). Unfortunately, from 1998 to 2003 the magnitude of the error in U3 discharge exceeds the magnitude of any outflow estimate, indicating that the volume changes only slightly, if at all. From the adjacent topography we can however infer that this lake is probably quite deep and like U2 contains water between subglacial floods.

3.1.3. Summary of mass budget 1996 to 2003

The destination lakes received a total of 1.08 ± 0.24 km³ from 1996 through 1998, a little under half of the 2.24 ± 0.5 km³ of water released by Lake L. Filling rates peaked 2–3 months after the peak discharge rate from Lake L (Table 2; Fig. 9). The maximum discharge rate of Lake L is approximately equal to the maximum combined filling rate of U1, U2 and U3 indicating that the three known destination lakes were at one point receiving all of the water flowing out of Lake L, and that it is unlikely that any of the water was flowing beyond U3 during this time. Later in 1998, Lake L continued to drain while Lakes U1, U2, and U3 had stopped inflating and the surface of U2 had begun to deflate. The only possible destination for the water that was still leaving Lake L would be to points downstream of U3. Overall, approximately 70% of the discharge from Lake L had made it downstream of Lake U3 by 2003. With knowledge of when and where water was flowing, we can construct a rudimentary water model with which to explain subglacial water flow between the lakes (Fig. 9).

3.2. Modeling of flow mechanisms

3.2.1. Semicircular ice-walled conduit

The rising limb of the hydrograph for Lake L can be replicated with a relatively simple model of a semicircular channel at the ice bed interface (Fig. 9). To replicate the maximum discharge and descending limb, it is necessary to include shoreline retreat in the model. Without shoreline retreat the modeled discharge grows indefinitely. With shoreline retreat the increasing distance and increasing elevation gain from the source lake to the next location downstream hinders the ability of the channel to continue melting its own opening, until creep closure dominates. The decreasing hydraulic gradient with time, however, appears responsible for the long duration of the descending limb of the flood hydrograph relative to the ascending limb. As such, the slope of the ice base and the lake bathymetry at the outlet exert a primary control on the evolution of discharge from the lake and may control the amount of water released from a given flood. In this respect Antarctic subglacial floods occurring over relatively low bedrock and ice-surface slopes demonstrate an increased sensitivity to subtle variations in bedrock topography. The subtle differences between the modeled and observed discharges with time may also result from neglecting change in lake area with time or departures in channel shape from a perfect semicircle.

Although the semicircular conduit model explains outlet dynamics fairly well it encounters increasing problems in describing water flow downstream, where the bedrock gradient becomes more adverse. As the energy gained from moving down gradient becomes insufficient to maintain water at the increasing pressure-melting point, some of the discharge must freeze onto the conduit walls. When ice begins to accrete on walls instead of melting, the only way to maintain a passage is for water pressure to exceed the overburden pressure or to flow in a distributed sheet along the ice/bed interface.

3.2.2. Broad, shallow canals in sediment

Using the relationship between sediment size and channel depth described in Parker (1978) with the assumed sediment size of 120–250 μm (Tulaczyk et al., 1998) and a discharge of 50 m³s⁻¹, we obtain channel dimensions of 0.1–0.4 m deep by 500–2000 m across. Given that the lateral dimensions greatly exceed those originally envisioned by Walder and Fowler (1994), it may be that we have several smaller braided canals rather than one single feature. The average water velocity in these canals would be on the order of 0.04 – 0.1 ms⁻¹, leading to travel time of 30 to 80 d between Lake L and the lowermost U lake. These travel times agree with the observed delay between the peak discharge of Lake L and the peak filling of the U lakes (Fig. 9). The estimated time required to close a canal at the Lake L outlet via viscous deformation is on the order of 300 d. The effective pressures at which a broad shallow canal closes are on the order of 20 kPa, equivalent to an elevation change of a few meters. These rates and values are all consistent observations of Lake L (Wingham et al., 2006). Although the semicircular channel is still a viable means of draining the Lake L, it appears that a flatter distributed system is in part responsible for the transportation of water during the Adventure Trench subglacial flood.

As a distributed system operating under water pressures fractions of a bar below the overburden pressure, the canal system readily adapts to channel contraction associated with the thermal accretion of ice both by redirection of water flow and erosion of new channels into the sediment along the sub-ice interface (Ng, 2000; Alley, 1989). Because the total ice–water contact area is significantly greater for a given discharge, the thickness of ice accreted and melted is significantly reduced, generally being on the order of 0.01 – 0.1 m a⁻¹ for the U lake system and locally as high as 0.2 m a⁻¹ at the outlet for U3.

4. Discussion

4.1. Lake retreat, thermal erosion and a distributed drainage

The AST discharge and other Antarctic subglacial discharge events differ from the jökulhlaups commonly observed in temperate glaciers primarily in that they begin and end at pressurized subglacial lakes and not subaerial lakes. The hydraulic head gradients associated with Antarctic floods are on the order of 0.1%–1%, two orders of magnitude less than their temperate counterparts. The relatively low hydraulic gradient leads to longer event duration, as channel growth and contraction are both relatively slow. Within this slow growth and decay it becomes possible to see the influences of lake bathymetry and ice draft on the discharge evolution. The lakes involved in Antarctic subglacial floods are typically far broader than they are deep. Consequently, shorelines may migrate many kilometers over the course of the filling and draining of the lake. Migrating shorelines may act both to limit the total discharge of a given event and may also play a role in the continued propagation of floodwater downstream. As the shoreline of a deflating lake will recede, the shoreline of an inflating lake will expand downstream. If water tends to collect immediately upstream of locations where the ratio of the basal slope to the surface slope inhibits thermal erosion by water traveling downstream, then the expansion of the lake shore downstream of such a barrier as a lake inflates may be the primary mechanism by which interior meltwater travels downstream through mountain ranges toward the onset of fast glacier flow.

Although we have demonstrated that the observed behavior of the outlet of Lake L can be roughly reproduced with a very simple conduit model, a broad distributed canal system appears to be more stable means of maintaining the flood downstream. The switch from a narrow conduit to a wide canal appears to take place close to the source lake outlet and consequently occurs early on, as the water from Lake L takes nearly three months to arrive at the destination lakes. It appears that maximum filling of the destination lakes was accomplished only after this canal was in place (Fig. 9). The transition between the conduit and a distributed water system is still a subject of debate (Flowers et al., 2003). The time lag between subsidence at Lake L and surface inflation at the destination lakes indicates that propagation of the flood was only possible under a distributed flow regime. This inference is further supported by departure of Lake L's discharge from the modeled discharge shortly after the destination lakes begin filling (Fig. 9). The paucity of lakes between Lake L and U1 indicates little, if any, water storage along the flow route (Carter et al., 2007). The deep bedrock valley constrains the flow path uniquely to the AST such that there are no side lakes that could be filled (Fig. 5).

The most difficult observation to reconcile with the distributed drainage system we have proposed for AST is the simultaneous filling of all three U lakes (Shoemaker, 2003). We can only conclude that whatever barriers existed between the three U lakes, they were not sufficient to prevent effectively instantaneous propagation of water pressure during the outburst. Again this may have been a consequence of high variability in local water pressures in the turbulent water flow of the discharge being more significant than the few meters of head difference separating the lakes. Alternatively the apparent head difference between the lakes may have been due to ice dynamical effects (Ridley et al., 1993). Variations in apparent hydraulic head of over 10 m have been observed in other large subglacial lakes (Studingner, 2007). Whether these are all separate or one single lake it was only after filling all three U lakes that the discharge was able to advance beyond U3. Once this advance began, the existence of an open pathway at the outlet of U3 was sufficient to allow partial drainage of the U2–U3 system, although the effect was most pronounced at U2 perhaps because of the greater width of U2 allowing for greater subsidence of the ice roof.

4.2. Flood initiation and termination at Lake L and U3

Fowler (1999) proposes that subglacial lake discharges commence by one of two mechanisms: simple flotation of the ice dam or thermal erosion of a conduit. We have demonstrated that a conduit enlarging via thermal erosion is a sustainable means of initiating discharge from Lake L, whereas such a conduit does not appear feasible for the exit of U3. According to our semicircular conduit model, an initial discharge of $1 \text{ m}^3 \text{ s}^{-1}$ would take nearly a year to enlarge to $3 \text{ m}^3 \text{ s}^{-1}$. Wingham et al. (2006) state that the filling rate for Lake L is likely on the order of 30 yr, based on a 1 mm/yr basal melt rate for the entire hydraulic catchment upstream. A more detailed analysis of melt rates for the uppermost reaches of this basin indicates that this figure is within bounds (Carter et al., in review). If the discharge from the catchment above Lake L is in steady state, then we can expect a base flow of about $3 \text{ m}^3 \text{ s}^{-1}$, and the 30-year repeat cycle for Lake L would be approximately correct (Wingham et al., 2006). However, a number of confirmed lakeless subglacial basins currently exist between Lake L and Lake Vincennes (Siegert and Ridley, 1998). These basins may have drained recently or have lower outlets, which as of yet have not been imaged in RES data (Remy et al., 2003). It is also possible that episodic discharge from Vincennes and lakes farther upstream may be significant to the filling of Lake L.

The ice–bedrock geometry immediately downstream of U3 does not favor thermal erosion of the ice, and, as such, sustaining a Rothlisberger channel would not be possible without significant heat advected from elsewhere. The relatively rapid filling rate of this lake, however, would favor hydraulic lifting of the roof. It is possible that as the roof inflated the lake shoreline expanded many kilometers downstream, perhaps even temporarily overtopping the inferred col from Adventure Trench to the next basin. As the lake ceiling lowered during discharge and the shoreline retreated below the bedrock col, ice would tend to accrete at the outlet and possibly close the outlet. Of any area along the flow path from Lake L to the most-downstream point known, Lake U3 should experience the highest rate of basal accretion (Alley et al., 1998). Given these high accretion rates, it is possible that the exit to Lake U3 was opened by pressurization of the lake, remained open throughout the drainage of U2, and then was closed by freezing around the outlet.

4.3. Hydraulic connections to the coast

Given that nearly 70% of the discharge reported for Lake L had moved beyond U3 by 2003, it is possible that some of this discharge reached coastal systems via the bedrock trenches of Byrd or Mulloch glaciers. The analysis of the hydraulic potential and surface data presented in this work indicates another possible lake 60 km downstream from U3 (Figs. 3 and 9). Unfortunately the available RES data downstream of this point does not allow for unique identification of a subglacial flow path, and so consequent discharge flow evolution is difficult to model realistically. The identification of other subglacial lakes within the Byrd and Mulloch basins, which may serve as possible destinations for future analysis of this basin, should focus on surface movement near these lakes, as the propagation and data from the GLAS/ICESat mission is favorable to resolving post-2003 surface motion downstream of U3, if such motion has occurred (Scambos et al., 2007).

The behavior of any lakes downstream is likely to be influenced not only by the catchment feeding the AST lakes, but by other catchments as well. Even within the study area there are several smaller basins, all of which likely contribute to the buildup and release of water from the lakes within and downstream (Fig. 5). The similarity between the 1974–75 shoreline and the 1999–2000 shoreline for Lake U2 suggests that these floods occur with regular frequency (Fig. 4). A more complete ice-thickness data set for the Byrd and Mulloch glacier catchments is required, however, to determine if and how interior subglacial water reaches the coast.

4.4. Impact of an intermittent distributed drainage system discharge on the motion of the overlying ice

The presence of a broad, shallow distributed canal system, such as the one modeled for this event, is expected to reduce basal friction and consequently enhance sliding of the overlying ice, possibly resulting in a temporary acceleration of ice flow in this region (Engelhardt et al., 1990). Such surges have been witnessed at other outlet glaciers, and enhanced flow has been proposed as taking place in the AST by at least one model for ice velocity (Wu and Jezek, 2004). The drawdown of the internal layers in the ice in this region suggests a relatively high rate of removal for basal ice (Fig. 4). The buckled layers are common to faster flow regions (Rippin et al., 2003; Siegert et al., 2004). Given, however, the low background ice-surface velocity of 1–10 m/yr for this area (Wu and Jezek, 2004), detecting a temporary flow acceleration on the order of a few tens of percent may prove difficult with current technology (Joughin et al., 1996).

4.5. Radar resolution of a distributed drainage system

Unlike semicircular conduits or R-channels, a distributed drainage system carrying 57–82 m³s⁻¹ will be on the order of hundreds of meters across and tens of centimeters deep and therefore should be observable in airborne RES data (Peters et al., 2005). Furthermore we expect such features to appear hydraulically flat in the radar images. A number of “fuzzy lakes” were identified in (Carter et al., 2007) along the hydraulic flow path upstream of the destination lake. A canal or sediment-rich braided stream of a depth less than 1 m would appear in the radar image as a bright feature with highly variable reflectivity along the flight line. Similarly, Popov and Masolov (2007) have imaged subglacial lakes near Vostok that had a significant hydraulic slope. Although radar reflections alone may not uniquely identify a particular subglacial water system it is possible to show that reflections are consistent with a given system if the discharge is known. By contrast a semicircular conduit would not be visible in radar images. It is possible that some “fuzzy lakes” and “indistinct lakes” as identified by Carter et al. (2007) may in fact be part of such a flow system or a remnant of such a flow system.

5. Conclusions

Within the AST, subglacial lakes downstream of Lake L received approximately 48% of the water released and delayed the progress of the discharge downstream by more than a year. When the discharge finally breached Lake U3, either by the expansion of the shoreline downstream past the seal or by simple roof flotation, it opened a passage that allowed the flow not only of the remaining floodwater from Lake L, but also approximately one-third of the water that had been previously stored in the U Lakes. Ultimately these lakes retained about 32% of the discharge from Lake L. Although these numbers are subject to considerable error, associated with uncertainties about the lake's shoreline outside the airborne RES coverage and surface flexure, it is safe to conclude that a significant fraction of the discharge from Lake L remained in the downstream AST lakes (Lakes U1, U2 and U3) and that a larger fraction made it to points farther downstream after the U lakes were full. With improved mapping of the ice thickness and continued collection of ice-surface motion data, it may be possible to track the progress of such an event to its termination point.

Although simple conduit physics explains the growth and decay of discharge from Lake L, it is necessary to employ a more sophisticated distributed drainage model to explain travel time and discharge evolution for points downstream. While several models for distributed drainage systems along a given flow line exist (Alley, 1989; Ng, 2000; Flowers et al., 2003; Flowers et al., 2004; Creyts, 2007), we found that the relatively simple Walder and Fowler (1994) model generally explained the flux evolution between the lakes with the

fewest introduced parameters, although some of the more recent models may prove more useful in calculating channel geometry. To realize the full potential of these more recent models, however, it would be necessary to get more observations on sediment transport in a low-gradient subglacial canal. With more information on the flow-path geometry, the material properties of the underlying sediments, and improved radar observations of the upper 120 km of the flow path, a more sophisticated model could be employed. Through such efforts it may be possible to better quantify the impact of subglacial discharge events on enhancing the flow of the overlying ice and quantifying sediment transport.

The AST discharge bears similarities to discharges observed in the fast-moving ice of the West Antarctic ice streams in terms of magnitude, hydraulic gradient and duration (Gray et al., 2005; Fricker et al., 2007). It is likely that the model we developed to explain the AST discharge event could be applied in these cases. The recurrence interval, however, is far less frequent than that of events closer to the coast. It is clear that every lake along a given discharge path will have its own effect on the progress of a subglacial discharge event.

Acknowledgements

The Support Office for Aerogeophysical Research at the University of Texas Institute for Geophysics, through which the data for this study was obtained, was funded by the National Science Foundation under Cooperative Agreement OPP 91-19379 and OPP 93-19379 as well as NSF grant OPP 99-11617. Additional data collection and processing was supported through NSF Grant OPP 96-15832 and OPP 98-14816. Multiple portions of this work were supported in part through the John A. and Katherine G. Jackson School of Geosciences Geology Foundation at The University of Texas at Austin and the Arthur E. Maxwell Graduate Fellowship. We thank Mr. James C. Patterson and Dr. James A. Austin for their support. Additional support for S.P.C. during the final write up of this work was provided by NSF Grant OCE 04-02363. Further financial and data support was provided by NASA grant NNX08AN68G. We also thank the Vetlesen Foundation for their generous financial support.

We thank the SOAR team members and collaborators. We thank Kevin Johnson, Steffen Saustrop, and Mark Weiderspan for their technical support in the processing of this data. We thank Marcy Davis, Jan Everett, Nancy Hard, Wilbert King, and Gwen Watson for administrative support. This manuscript was improved with comments from Dr. David Mohrig, Susan Carter, Charles Jackson, Helen A. Fricker, Joseph A. Walder, Anthony Wild, and one anonymous reviewer.

Appendix A. Supplementary data

Supplementary data associated with this article can be found, in the online version, at [doi:10.1016/j.epsl.2009.03.019](https://doi.org/10.1016/j.epsl.2009.03.019).

References

- Alley, R.B., 1989. Water-pressure coupling of sliding and bed deformation: I. Water system. *J. Glaciol.* 35, 108–118.
- Alley, R.B., Lawson, D.E., Evenson, E.B., Strasser, J.C., Larson, G.J., 1998. Glaciohydraulic supercooling: a freeze-on mechanism to create stratified, debris-rich basal ice: II. Theory. *J. Glaciol.* 44, 563–569.
- Arthern, R.J., Wingham, D.J., Ridout, A.L., 2001. Controls on ERS altimeter measurements over ice sheets: Footprint-scale topography, backscatter fluctuations, and the dependence of microwave penetration depth on satellite orientation. *J. Geophys. Res.-Atmos.* 106, 33471–33484.
- Arthern, R.J., Winebrenner, D.P., Vaughan, D.G., 2006. Antarctic snow accumulation mapped using polarization of 4.3-cm wavelength microwave emission. *J. Geophys. Res.-Atmos.* 111.
- Bamber, J., Gomez-Dans, J.L., 2005. The accuracy of digital elevation models of the Antarctic continent. *Earth Planet. Sci. Lett.* 237, 516–523. [doi:10.1016/j.epsl.2005.10.06](https://doi.org/10.1016/j.epsl.2005.10.06).
- Bell, R.E., 2008. The role of subglacial water in ice-sheet mass balance. *Nat. Geosci.* 1, 297–304.

- Bell, R.E., Studinger, M., Fahnestock, M.A., Shuman, C.A., 2006. Tectonically controlled subglacial lakes on the flanks of the Gamburtsev Subglacial Mountains, East Antarctica. *Geophys. Res. Lett.* 33 (L02402). doi:10.1029/2005GL025207.
- Bell, R.E., Studinger, M., Shuman, C.A., Fahnestock, M.A., Joughin, I., Ian, 2007. Large subglacial lakes in East Antarctica at the onset of fast-flowing ice streams. *Nature* (London) 445, 904–907. doi:10.1038/nature05554.
- Blankenship, D.D., Morse, D.L., Finn, C.A., Bell, R.E., Peters, M.E., Kempf, S.D., Hodge, S.M., Studinger, M., Behrendt, J.C., Brozena, J.M., 2001. Geologic controls on the initiation of rapid basal motion for West Antarctic ice streams; a geophysical perspective including new airborne radar sounding and laser altimetry results. In: Alley, R.B., Bindschadler, R.A. (Eds.), *West Antarctic Ice Sheet: Behavior and Environment*. Antarctic Research Series, vol. 77, pp. 105–121.
- Björnsson, H., 1992. Jökulhlaups in Iceland; prediction, characteristics and simulation. *Ann. Glaciol.* 16, 95–106.
- Bougamont, M., Tulaczyk, S., Joughin, I., 2003. Numerical investigations of the slow-down of Whillans Ice Stream. In: Duval, P. (Ed.), *West Antarctica: is it shutting down like Ice Stream C?* pp. 239–246.
- Carter, S.P., Blankenship, D.D., Peters, M.E., Young, D.A., Holt, J.W., Morse, D.L., 2007. Radar-based subglacial lake classification in Antarctica. *Geochem. Geophys. Geosyst.* 8 (Q03016). doi:10.1029/2006GC001408.
- Catania, G., Paola, C., 2001. Braiding under glass. *Geology* 29, 259–262. doi:10.1130/0091-7613(2001)029-0259:2.0.CO;2.
- Clarke, G.K.C., 2003. Hydraulics of subglacial outburst floods: new insights from the Spring-Hutter formulation. *J. Glaciol.* 49, 299–313.
- Clarke, G.K.C., 2005. Subglacial processes. *Ann. Rev. Earth Planet. Sci.* 33 <http://arjournals.annualreviews.org/doi/pdf/10.1146/annurev.earth.33.092203.122621>.
- Clarke, G.K.C., 2006. Nye lecture: water under ice: curiosities, complexities, and catastrophes. *Eos Trans. AGU* 87 Abstract C23A-01.
- Creys, T., 2007. A numerical model of glaciohydraulic supercooling: thermodynamics and sediment entrainment. Ph.D thesis, University of British Columbia.
- Denton, G.H., Sugden, D.E., 2005. Meltwater features that suggest Miocene ice-sheet overriding of the Transantarctic Mountains in Victoria Land, Antarctica. *Geogr. Ann.* A 87A, 67–85. doi:10.1111/j.0435-3676.2005.00245.x.
- DiMarzio, J., Brenner, A., Schutz, R., Shuman, C.A., Zwally, H.J., 2007. GLAS/ICESat 500 m laser altimetry digital elevation model of Antarctica. National Snow and Ice Data Center, Boulder, Colorado, USA, Digital Media.
- Drewry, D.J., 1975. Radio echo sounding map of Antarctica (~90°E–180°). *Polar Rec.* 17, 359–374.
- Engelhardt, H., Humphrey, N., Kamb, B., Fahnestock, M., 1990. Physical conditions at the base of a fast moving Antarctic ice stream. *Science* 248, 57–59.
- Evatt, G.W., Fowler, A.C., 2007. Cauldron subsidence and subglacial floods. *Ann. Glaciol.* 45, 163–168.
- Evatt, G.W., Fowler, A.C., Clark, C.D., Hulton, N.R.J., 2006. Subglacial floods beneath ice sheets. *Philos. Trans. R. Soc. Lond. Ser. A* 364, 1769–1794.
- Ferraccioli, F.C., Bozzo, E., Zanolla, C., Gandolfi, S., Tabacco, I.E., Frezzotti, M., 2002. Rifted crust at the East Antarctic Craton margin; gravity and magnetic interpretation along a traverse across the Wilkes subglacial basin region. *Earth Planet. Sci. Lett.* 192, 407–421. doi:10.1016/S0012-821X(01)00459-9.
- Flowers, G.E., Björnsson, H., Palsson, F., 2003. New insights into the subglacial and periglacial hydrology of Vatnajökull, Iceland, from a distributed physical model. *J. Glaciol.* 49, 257–270.
- Flowers, G.E., Björnsson, H., Palsson, F., Clarke, G.K.C., 2004. A coupled sheet-conduit mechanism for Jökulhlaup propagation. *Geophys. Res. Lett.* 31. doi:10.1029/2003GL019088.
- Fowler, A.C., 1999. Breaking the seal at Grimsvotn, Iceland. *J. Glaciol.* 45, 506–516.
- Fowler, A.C., Ng, F.S., 1996. The role of sediment transport in the mechanics of Jökulhlaups. *Ann. Glaciol.* 22, 255–259.
- Fricker, H.A., Scambos, T., Bindschadler, R., Padman, L., 2007. An active subglacial water system in West Antarctica mapped from space. *Science* 315, 1544–1548. doi:10.1126/science.1136897.
- Fricker, H., Scambos, A.T., 2009. Connected subglacial lake activity on lower Mercer and Whillans Ice Streams, West Antarctica, 2003–2008. *Journal of Glaciology* 20, 303–315.
- Goodwin, I.D., 1988. The nature and origin of a jökulhlaup near Casey Station, Antarctica. *J. Glaciol.* 34, 95–101.
- Gorman, M.R., Siegert, M.J., 1999. Penetration of Antarctic subglacial water masses by VHF electromagnetic pulses: estimates of minimum water depth and conductivity. *J. Geophys. Res.* 104, 29,311–29,320. doi:10.1029/1999JB900271.
- Gray, L., Joughin, I., Tulaczyk, S., Spikes, V.B., Bindschadler, R., Jezek, K., 2005. Evidence for subglacial water transport in the West Antarctic ice sheet through three-dimensional satellite radar interferometry. *Geophys. Res. Lett.* 32. doi:10.1029/2004GL021387.
- Haran, T., Bohlander, J., Scambos, T., Fahnestock, M., 2005. compilers, MODIS Mosaic of Antarctica (MOA) Image Map. National Snow and Ice Data Center, Boulder, CO, USA. Digital media.
- Hooke, R.L., 1998. *Principles of Glacier Mechanics*. Prentice Hall, New Jersey. 248 pp.
- Hooke, R.L., Laumann, T., Kohler, J., 1990. Subglacial water pressures and the shape of subglacial conduits. *J. Glaciol.* 36, 67–71.
- Johnson, J.V., 2002. A basal water model for ice sheets, Ph.D Thesis, University of Maine.
- Joughin, I., Kwok, R., Fahnestock, M., 1996. Estimation of ice-sheet motion using satellite radar interferometry: method and error analysis with application to Humboldt Glacier, Greenland. *Journal of Glaciology* 42, 564–575.
- Kamb, B., 1987. Glacier surge mechanism based on linked cavity configuration of the basal water conduit system. *Journal of Geophysical Research-Solid Earth and Planets* 92, 9083–9100.
- Le Brocq, A.M., Payne, A.J., Siegert, M.J., 2006. West Antarctic balance calculations: Impact of flux-routing algorithm, smoothing algorithm and topography. *Comput. Geosci.* 32, 1780–1795.
- Lythe, M.B., Vaughan, D.G., 2001. BEDMAP: a new ice thickness and subglacial topographic model of Antarctica. *J. Geophys. Res.-Solid Earth* 106, 11335–11351. doi:10.1029/2000JB900449.
- Ng, F.S.L., 2000. Canals under sediment-based ice sheets. *Ann. Glaciol.* 30, 146–152.
- Nye, J.F., 1976. Water flow in glaciers, jökulhlaups, tunnels and veins. *J. Glaciol.* 17, 181–207.
- Pattyn, F., 2003. A new three-dimensional higher-order thermomechanical ice sheet model: Basic sensitivity, ice stream development, and ice flow across subglacial lakes. *J. Geophys. Res.* 108 (B8), 2382. doi:10.1029/2002JB002329.
- Parker, G., 1978. self-formed straight rivers with equilibrium banks and mobile bed .1. Sand-silt river. *J. Fluid Mech.* 89, 109–125.
- Payne, A.J., Holland, P.R., Shepherd, A.P., Rutt, I.C., Jenkins, A., Joughin, I., 2007. Numerical modeling of ocean-ice interactions under Pine Island Bay's ice shelf. *J. Geophys. Res.-Oceans* 112. doi:10.1029/2006JC003733.
- Peters, M.E., Blankenship, D.D., Morse, D.L., 2005. Analysis techniques for coherent airborne radar sounding: application to West Antarctic ice streams. *J. Geophys. Res.* 110. doi:10.1029/2004JB003222.
- Peters, L.E., Anandakrishnan, S., Alley, R.B., Smith, A.M., 2007. Extensive storage of basal meltwater in the onset region of a major West Antarctic ice stream. *Geology* 25, 251–254. doi:10.1130/G23222A.23221.
- Popov, S.V., Masolov, V.N., 2007. Forty-seven new subglacial lakes in the 0–110° E sector of East Antarctica. *Journal of Glaciology* 53, 289–297. doi:10.3189/172756507782202856.
- Remy, F., Legresy, B., 2004. Subglacial hydrological networks in Antarctica and their impact on ice flow. *Annals of Glaciology* 39, 67–72. doi:10.3189/172756404781814401.
- Remy, F., Testut, L., Legresy, B., Forieri, A., Bianchi, C., Tabacco, I.E., 2003. In: Duval, P. (Ed.), *Lakes and subglacial hydrological networks around Dome C, East Antarctica*, pp. 252–256.
- Richter, T.G., Holt, J.W., Blankenship, D.D., 2001. Airborne gravimetry over the Antarctic ice sheet, Proceedings of the International Symposium on Kinematic Systems in Geodesy. *Geomat. Navig.*
- Ridley, J.K., Cudlip, W., Laxon, S.W., 1993. Identification of subglacial lakes using ERS-1 Radar Altimeter. *J. Glaciol.* 39, 625–634.
- Rippin, D., Siegert, M.J., Bamber, J.L., 2003. The englacial stratigraphy of Wilkes Land, East Antarctica, as revealed by internal radio-echo sounding layering, and its relationship with balance velocities. *Ann. Glaciol.* 36, 189–196.
- Roberts, M.J., 2005. Jökulhlaups: a reassessment of floodwater flow through glaciers. *Rev. Geophys.* 43. doi:10.1029/2003RG000147.
- Röthlisberger, H., 1972. Water pressure in intra- and subglacial channels. *J. Glaciol.* 11, 177–203.
- Scambos, T.A., Haran, T.M., Fahnestock, M.A., Painter, T.H., Bohlander, J., 2007. Continent-wide surface morphology and snow grain size. *Remote Sens. Environ* 30 (2–3), 242–257. doi:10.1016/j.rse.2006.12.020.
- Sergienko, O.V., MacAyeal, D.R., Bindschadler, R.A., 2007. Causes of sudden, short-term changes in ice-stream surface elevation. *Geophys. Res. Lett.* 34.
- Shoemaker, E.M., 2003. Effects of bed depressions upon floods from subglacial lakes. *Glob. Planet. Change* 35, 175–184. doi:10.1016/S0921-8181(02)00125-X.
- Shuman, S.H., Zwally, H.J., Schultz, B.E., Brenner, A.C., DiMarzio, J.P., Suchdeo, V.P., Fricker, H.A., 2006. ICESat Antarctic elevation data: Preliminary precision and accuracy assessment. *Geophysical Research Letters* 33, L07501. doi:10.1029/2005GL025227.
- Siegert, M.J., Ridley, J.K., 1998. Determining basal ice-sheet conditions in the Dome C region of East Antarctica using satellite radar altimetry and airborne radio-echo sounding. *Journal of Glaciology* 44, 1–8.
- Siegert, M.J., Welch, B., Morse, D.L., Vieli, A., Blankenship, D.D., Joughin, I., King, E.C., Vieli, G.J., Leysinger, J.M.C., Payne, A.J., Jacobel, R., 2004. Ice flow direction change in interior West Antarctica. *Science* 305, 1948–1951. doi:10.1126/science.1101072.
- Siegert, M.J., Carter, S.P., Tabacco, I.E., Popov, S., Blankenship, D.D., 2005. A revised inventory of Antarctic subglacial lakes. *Antarct. Sci.* 17, 453–460.
- Smith, B.E., Raymond, C.F., Scambos, T., 2006. Anisotropic texture of ice sheet surfaces. *J. Geophys. Res.* 111 (F01019). doi:10.1029/2005JF003393.
- Stearns, L.A., Smith, B.E., Hamilton, G.S., 2008. Increased flow speed on a large East Antarctic outlet glacier caused by subglacial floods. *Nat. Geosci.* 1, 827–831.
- Studinger, M., Bell, R.E., Buck, R.W., Karner, G.D., Blankenship, D.D., 2004. Sub-ice geology inland of the Transantarctic Mountains in light of new aerogeophysical data. *Earth Planet. Sci. Lett.* 220, 391–408. doi:10.1016/S0012-821X(04)00066-4.
- Studinger, M., 2007. Estimating the salinity of subglacial lakes from aerogeophysical data. Open File Report U. S. Geological Survey, Report: OF 032.
- Tulaczyk, S., Kamb, B., Scherer, R.P., Engelhardt, H.F., 1998. Sedimentary processes at the base of a West Antarctic ice stream; constraints from textural and compositional properties of subglacial debris. *J. Sediment. Res.* 68, 487–496.
- Tulaczyk, S., Kamb, W.B., Engelhardt, H.F., 2000. Basal mechanics of Ice Stream B, West Antarctica 2. Undrained plastic bed model. *J. Geophys. Res.-Solid Earth* 105, 483–494.
- Vogel, S.W., Tulaczyk, S., 2006. Ice-dynamical constraints on the existence and impact of subglacial volcanism on West Antarctic ice sheet stability. *Geophys. Res. Lett.* 33. doi:10.1029/2006GL027345.
- Walder, J.S., Fowler, A., 1994. Channelized subglacial drainage over a deformable bed. *J. Glaciol.* 40, 3–15.
- Wingham, D.J., Siegert, M.J., Shepherd, A., Muir, A.S., 2006. Rapid discharge connects Antarctic subglacial lakes. *Nature* 440, 1033–1036. doi:10.1038/nature04660.
- Wu, X., Jezek, Kenneth C., 2004. Antarctic ice-sheet balance velocities from merged point and vector data. *J. Glaciol.* 50, 219–230.